# STUDY OF WIND FARM BEHAVIOUR DURING POWER SYSTEM NETWORK DISTURBANCE

T. R. Ayodele, A. A. Jimoh, J. L. Munda and J. T. Agee
*Department of Electrical Engineering, Tshwane University of Technology, Pretoria, South Africa*

Keywords: Wind farm, Doubly fed induction generator, Power system, Disturbance.

Abstract: This paper studies the impact of disturbances emanating from the power system network on the behaviour of a wind farm (WF) consisting of doubly fed induction generator (DFIG). Response of the WF to disturbances like fault occurence, sudden change in load, sudden loss of transmission line and loss of generation are considered in the study. The models of various systems making up the wind conversion system are presented. Pitch control system is used for the stabilization of the wind turbine against the disturbances. Parts of the key results show that the generator inertia, converter controller and types of disturbance have significant effect on the response of a WF.



## 1 INTRODUCTION

A lot of efforts are geared towards grid integration of renewable energies as a result of environmental concern and energy security. Among these renewable energies, wind energy stands out as it has the ability to produce electricity in the MW range. At present, the wind power growth rate stands at 20% annually and it is predicted that 12% of the world electricity may come from wind power by the year 2020 (El-Sayed, 2010). There is tendency to surpass this rate with the present advancement in the offshore wind farm techologies.

There are various types of wind turbines in use around the world each having its own advantages and disadvantages (Slootweg et al., 2001). The most used one is the variable speed wind turbine with doubly fed induction generator (DFIG) due to the numerous advantages it offers over others et al., 2005).

The behaviour and the characteristic of the conventional generators for electricity generation are well known by the utility operators. With the advent of wind power, different types of generator technologies are introduced to the power system. This poses a lot of concern to most utility operators as the response of these generators to network disturbance is not well understood.

Most existing literature is focused on the analysis of the behavior of power system network as a result of wind farm integration (Eping et al., 2005; Xing et al., 2005; Naimi and Bouktir 2008; Folly and Sheetekela, 2009). This paper looks at it from the other angle by studying the response of the wind farm to disturbance in the power system network. The study is limited to Wind farm (WF) consisting of variable speed DFIG.

The structure of the remaing part of the paper is as follows, section two presents the model of the wind conversion system made of variable speed DFIG. Section three describes the system under study. Simulation results obtained are discussed in section 4 while section five presents the conclusion.

## 2 MODELLING OF DFIG WIND CONVERSION SYSTEM

Wind conversion system comprises of the aerodynamic system, the mechanical shaft system, electrical system of the induction generator, the pitch control system, the speed control system, the rotor side converter controller and the grid side converter controller. All these systems are combined together to form a unit system of a wind farm.

### 2.1 Aerodynamic Torque Model

Aerodynamic model involves the extraction of

Ayodele T., Jimoh A., Munda J. and Agee J..
STUDY OF WIND FARM BEHAVIOUR DURING POWER SYSTEM NETWORK DISTURBANCE.
DOI: 10.5220/0003576202410248
In *Proceedings of 1st International Conference on Simulation and Modeling Methodologies, Technologies and Applications* (SIMULTECH-2011), pages 241-248
ISBN: 978-989-8425-78-2

useful mechanical power from the available wind power. Available wind power is given by

$$P_{wind} = \frac{1}{2}\rho\pi R^2 V^3 \quad (1)$$

where $P_{wind}$, $\rho$, $R$ and $V$ are the available power in the wind, air density, radius of the turbine blade and the wind speed that reaches the rotor swept area. The fraction of wind power that is converted to the turbine mechanical power $P_m$ is given by

$$P_m = \frac{1}{2}\rho\pi R^2 C_p(\lambda,\beta) V^3 \quad (2)$$

where $C_p$ gives the fraction of available wind power that is converted to turbine mechanical power, $\lambda$ and $\beta$ are the tip speed ratio and the pitch angle respectively. The $C_p$, $\lambda$ and $\beta$ are related by equation 3 and 4 (El-Sayed and Adel, 2010)

$$C_p(\lambda,\beta) = c_1\left(\frac{c_2}{\lambda_i} - c_3\beta - c_4\right)e^{\frac{c_5}{\lambda_i}} + c_6\lambda \quad (3)$$

$$\frac{1}{\lambda_i} = \frac{1}{1+0.08\beta} - \frac{0.035}{\beta^2+1} \quad (4)$$

Given $c_1$=0.5176, $c_2$=116, $c_3$=0.4, $c_4$=5, $c_5$=21 and $c_6$=0.0068 ,the relationship between $C_p$ against $\lambda$ at various $\beta$ is given in figure 1

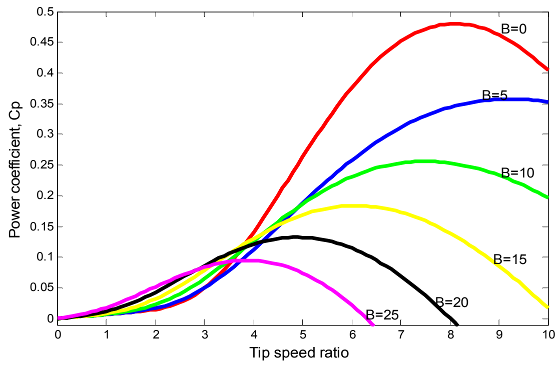


Figure 1: Relationship between Power coeficient and tip speed ratio at different pitch angle.

The tip speed ratio is given by (5)

$$\lambda = \frac{R\omega t}{V} \quad (5)$$

The mechanical torque developed by the wind power

$$T_m = \frac{P_m}{\omega_t} = \frac{\frac{1}{2}\rho\pi R^2 C_p(\lambda,\beta)V^3}{\omega_t} \quad (6)$$

where $\omega_t$ is the turbine speed.

For efficient wind power capture by the variable wind turbine (Arifujjaman et al., 2009), $\lambda = \lambda_{opt}$, therefore (5) can be re-written as

$$V = \frac{R\omega t}{\lambda_{opt}} \quad (7)$$

subtituting (7) in (6), Optimum torque can be obtained

$$T_{opt} = \frac{P_{opt}}{\omega_t} = \frac{\frac{1}{2}\rho\pi R^2 C_p(\lambda_{opt},\beta)R^3}{\omega_t(\lambda_{opt})^3} \quad (8)$$

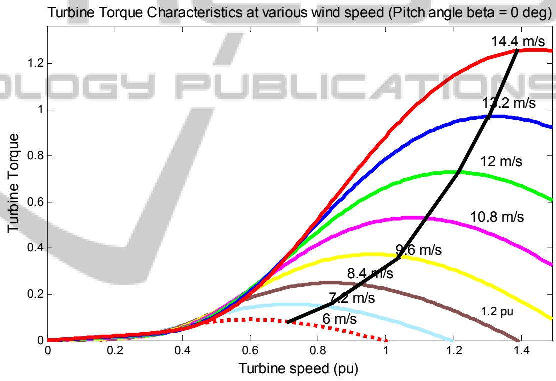


Figure 2: Maximum torque tracking of a variable speed wind turbine.

## 2.2 The Mechanical Shaft System Model

Adequate model of the mechanical drive train is required when the study involves the response of a system to heavy disturbances. It is better to represent the shaft by at least two- mass model (Poller, 2009). Model of the shaft system with two mass models is presented. The turbine is coupled to the generator through a gearbox as shown in figure 3

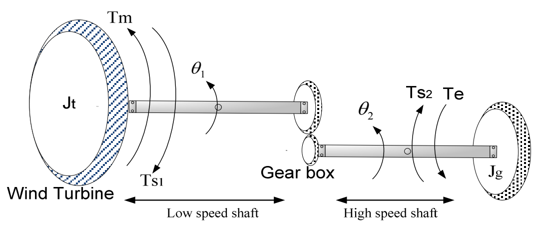


Figure 3: Two mass model of the mechanical shaft system.

From the figure, the following equations can be derived (9)-(16)

$$2H_t \frac{d\omega_t}{dt} = T_m - Ts_1 \quad (9)$$

$$2Hg \frac{d\omega_r}{dt} = Ts_2 - T_e \quad (10)$$

where

$$H_g = \frac{J_g \omega^2}{2{n_p}^2 P_g} \text{ and } H_T = \frac{J_T \omega^2}{2n^2 P_g} \quad (11)$$

$$Ts_1 = K_1\theta_1 - F_1 \frac{d\theta_1}{dt} \text{ and } Ts_2 = K_2\theta_2 - F_2 \frac{d\theta_2}{dt} \quad (12)$$

$$\theta_{eq} = \theta_1 - \theta_2, \quad K_{eq} = \frac{K_1 * K_2}{K_1 + K_2}, \quad T_{eq} = \frac{Ts_1 * Ts_2}{Ts_1 + Ts_2} \quad (13)$$

$$T_{eq} = K_{eq}\theta_{eq} + F_{eq}\frac{d\theta_{eq}}{dt} \quad (14)$$

$$\frac{d\theta_{eq}}{dt} = \omega_t - \omega_r \quad (15)$$

$$\frac{\mathrm{d}\theta_{\mathrm{eq}}}{\mathrm{dt}} = \omega_{\mathrm{t}} - \omega_{\mathrm{r}} \quad (16)$$

where $H_t$, $Hg$ are the pu turbine and generator inertia respectively. $J_g$ and $J_T$ are the inertia in kgm$^2$. $T_e$ is the electromechanicl torque developed by the induction generator, $T_m$ is the pu mechanical torque applied to the turbine by the wind as given in (5) . $Ts_1$, $Ts_2$ , $T_{eq}$ are the torques developed by the shaft at the low speed side, torque developed by the shaft at the high speed side and the equivalent torque developed by the shafts respectively. $\omega_t$ and $\omega_r$ are the pu turbine and generator rotor speed. $K_1$, $K_2$ and $K_{eq}$, are shaft stiffness at low speed side, shaft stiffness at high speed side and the total shaft stiffness. $F_1$, $F_2$ and $F_{eq}$ are the damping coefficient of the shaft at the low speed side, high speed side and the equivalent damping coefficient of the shaft respectively. $\theta_1$, $\theta_2$ and $\theta_{eq}$ are the angle of twist of the shaft at low speed, high speed and the equivalent angle of twist of the shaft respectively. $n_p$ is the number of pole pair, $n$ is the gear ratio, $P_g$ is the generator active power, $\omega$ is $2\pi f$ where $f$ is the frequency.

## 2.3 Pitch Angle Controller Model

Pitch angle controller majorly serves a purpose of limiting the generated power to the rated power in the time of high wind speed. It also limits the speed of the generator during heavy disturbances. The pitch controller based on PI is given by (17) (El-Sattar et al., 2008)

$$\frac{d\beta}{dt} = \frac{1}{\tau_s}\left(\beta_{ref} - \beta\right)$$
$$\beta_{ref} = \left(k_P + \frac{k_i}{s}\right)\left(P_{ref} - P_m\right) \quad (17)$$

where $\beta_{ref}$ is the reference pitch control, $k_P$ and $k_i$ are the proportional and integral parameter of the PI controller, $P_{ref}$ is the reference turbine power

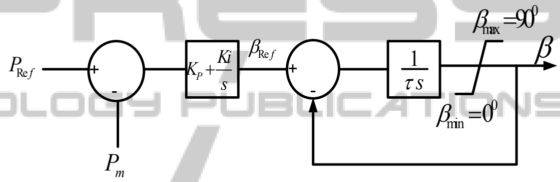


Figure 4: Pitch angle controller.

## 2.4 Wind Generator Model

Most wind farms are made of induction generators because they are cheap and robust. The dq stator and rotor voltage equations model in generating mode are as follows (Lipo 2000; Krause et al., 2002). The equation presented is a fifth order model. Third order model is obtained by neglecting the transient term in the stator voltage equation.

$$v_{qs} = -r_s i_{qs} - \omega\lambda_{qs} - p\lambda_{qs} \quad (18)$$

$$v_{ds} = -r_s i_{ds} + \omega\lambda_{qs} - p\lambda_{ds} \quad (19)$$

$$v_{qr} = -r_r i_{qr} - \left(\omega - \omega_r\right)\lambda_{qr} - p\lambda_{qr} \quad (20)$$

$$v_{dr} = -r_r i_{dr} + \left(\omega - \omega_r\right)\lambda_{qr} - p\lambda_{dr} \quad (21)$$

where $r_s$, $r_r$ are the stator and rotor speed resistance, $p$ is $\frac{d(.)}{dt}$ term.

The stator and rotor flux equations are

$$\lambda_{qs} = L_s i_{qs} + L_m i_{qr} \quad (22)$$

$$\lambda_{ds} = L_s i_{ds} + L_m i_{dr} \quad (23)$$

$$\lambda_{qr} = L_r i_{qr} + L_m i_{qs} \tag{24}$$

$$\lambda_{dr} = L_r i_{dr} + L_m i_{ds} \tag{25}$$

where $L_s$, $L_r$, $L_m$ are the stator, rotor and magnetzing inductance respectively. $i_{ds}$, , $i_{qs}$ $i_{dr}$ and $i_{qr}$ are the stator and rotor d-axis and q-axis.

The electromechanical torque, $T_e$ developed by the induction generator in pu can be derived as (26) given by

$$T_e = \frac{1}{\sigma}\left(\lambda_{qs}\lambda_{dr} - \lambda_{qr}\lambda_{ds}\right) \tag{26}$$

where $\sigma = 1 - \dfrac{L_m^2}{L_r L_s}$

The equation is completed by the mechanical coupling equation in pu between the turbine and the generator using two mass model as derived in (9)-(16)

$$\frac{d\omega_r}{dt} = \frac{1}{2H_g}\left(Ts_2 - T_e\right)$$

the active and reactive power generated by the induction generator is given as

$$P_s = \frac{3}{2}\left(v_{qs} i_{qs} + v_{ds} i_{ds}\right) \tag{27}$$

$$Q_s = \frac{3}{2}\left(v_{qs} i_{ds} - v_{ds} i_{qs}\right) \tag{28}$$

## 2.5 Grid Connection of DFIG Wind Farm

DFIG technology makes use of wound rotor. The stator is directly connected to the grid while the rotor is coupled to the grid through a Pulse width modulation (PWM) frequency converter as shown in figure 4. The converter carries only the rotor slip power typically in the range of 10-15% of the generated power (Veganzones et al., 2005).

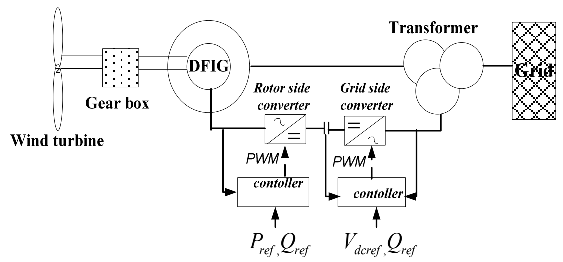


Figure 5: DFIG with PWM converter control system.

For dynamic study of DFIG, the converter controller model is important. Stator flux oriented control is commonly used in the decoupled control of DFIG.

## 2.6 DFIG Rotor Side Converter Controller

The control of the DFIG rotor is done in a synchronous rotating reference frame i.e $\omega = \omega_e$ in equation (18)-(21). The rotor side converter controls the stator active and reactive power of the DFIG. By alligning the dq reference frame in the stator flux reference frame, then $v_{ds} = 0$, $v_{qs} = v_s$, $\lambda_{qs} = 0$ and $\lambda_{ds} = \lambda_s$. Subtituting these in (22)-(25), (27), (28) and re-arranging, we obtain

$$P_s = -\frac{3}{2}\frac{L_m}{L_s} v_s i_{qr}^* \tag{29}$$

$$Q_s = \frac{3}{2L_s}\left(\frac{v_s^2}{\omega_s} - v_s L_m i_{dr}^*\right) \tag{30}$$

The rotor voltage equation governing the active and reactive power control can be obtained by rearranging equation (18)-(25) and is given by (31) and (32) (Krause et al., 2002)

$$v_{dr}^* = \left(k_{dp} + \frac{k_{di}}{s}\right)\left(i_{dr}^* - i_{dr}\right) - \left(\omega_e - \omega_r\right)\sigma L_r i_{qr} \tag{31}$$

$$v_{qr}^* = \left(k_{qp} + \frac{k_{qi}}{s}\right)\left(i_{qr}^* - i_{qr}\right) + \left(\omega_e - \omega_r\right)\left(\sigma L_r i_{dr} - \frac{L_m}{L_s}\lambda_S\right) \tag{32}$$

where, $k_{dp}$, $k_{di}$ are the PI proportional and integral constant for the d-axis for the control of reactive power while gain $k_{qp}$, $k_{qi}$ are the PI constant for controlling the active power. $i_{qr}^*$ and $i_{dr}^*$ are the reference current for the active and reactive power respectively. $v_{dr}^*$ and $v_{qr}^*$ are the dq reference voltage which will be converted to a-b-c frame to generate command for the rotor end PWM converter. The block diagram is shown in figure 6a and 6b

## 2.7 DFIG Grid Side Converter Controller

The main objective of grid side controller is to maintain the dc link between the back to back PWM converters at constant voltage irrespective of the direction of power flow (Krause et al., 2002). The dq

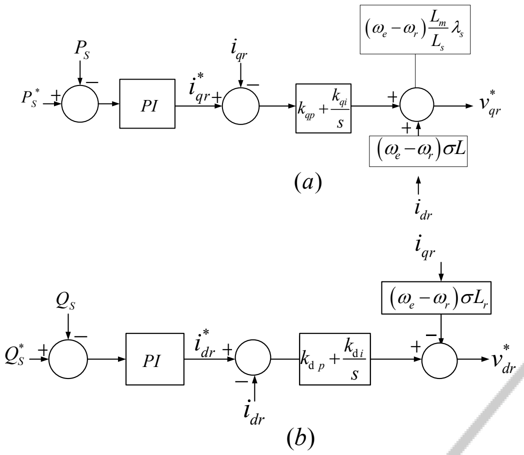

Figure 6: Rotor side Controller system.

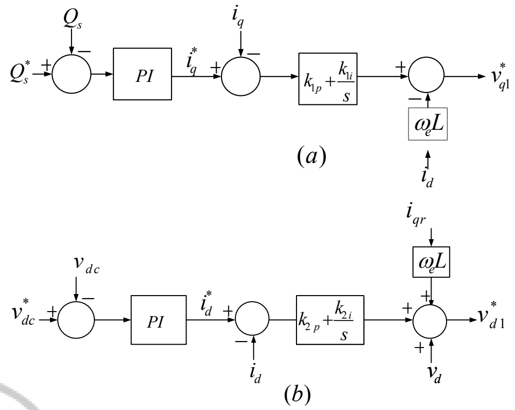

Figure 7: Grid side controller system.

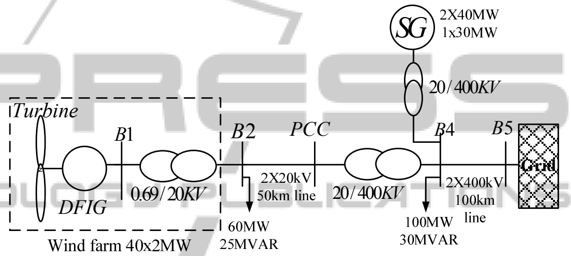


Figure 8: The system under study.

voltage for the grid side converter is represented by (33) (Soares et al., 2009)

$$
\begin{aligned}
v_q &= Ri_q + L\frac{di_q}{dt} + \omega_e L_{id} + v_{q1} \\
v_d &= Ri_d + L\frac{di_d}{dt} - \omega_e L_{iq} + v_{d1}
\end{aligned}
\tag{33}
$$

Re-arranging 33 with $v_{qs} = 0$, the governing voltage equation for the grid side converter can be obtained

$$
\begin{aligned}
v_{q1}^* &= -\left(k_{1p} + \frac{k_{1i}}{s}\right)\left(i_q^* - i_q\right) - \omega_e L_{id} \\
v_{d1}^* &= -\left(k_{2p} + \frac{k_{2i}}{s}\right)\left(i_d^* - i_d\right) + \omega_e L_{iq} + v_d
\end{aligned}
\tag{34}
$$

where $k_{1p}$, $k_{1i}$ are the q axis PI propornal and the integral constant. $k_{2p}$, $k_{2i}$ are the d axis PI proportionality and integral constant respectively. $v_{q1}^*$ and $v_{d1}^*$ are the reference voltage that generates the command for the grid side PWM converter after conversion to abc frame. $i_q^*$ is derived from the grid reactive power error while $i_d^*$ is derived from the dc link voltage error as shown in figure 7a and 7b respectively.

## 3 SYSTEM UNDER STUDY

The system considered for the study is shown in figure 8. It consists of 110MW, 50MVAR synchronous generator (SG) connected to bus 4 through a 20/400kV transformer.

The wind farm (WF) is made up of 40 wind turbines of 2MW, 0.69kV each modelled as an aggregate wind turbine. Aggregate model reduces simulation time required by detailed multi turbine system (Conroy and Watson 2009). It is assumed that the wind farms are located far from the point of common connection (PCC) where the wind resources are abundantly located as the case for most real wind farms. The WF is connected to the PCC through two 20km line (to allow disconnection of a line) and 69/20KV transformer. The WF is feeding a 60MW, 25MVAR local load connected to bus2 (B2). Another 100MVA, 30MVAR load is connected to the high voltage bus (B4). The whole system is connected to a strong grid through a two 400kV, 100km transmission lines.

## 4 THE SIMULATION RESULT AND DISCUSSION

Different scenarios were created to get insight into the response of WF to disturbances from the grid.

First, the response of the wind farm was studied when there is a step change of 20% in the local load connected to B2 at 1s. The results with the rotor controller in place and out of place are depicted in figure 9. From the figure it can be observed that with the controller in place, the active power (the negative values indicate a power injected into the grid) and the electrical torque are immediately returned to the pre-disturbance level. The step increase in the local load resulted in a dip in the terminal voltage and an increase in the speed of the generator, however, it stabilizes to a new value almost immedately. This is as a result of change in the system configuration. With the rotor controller out, the system is stable but it takes about 3s for the wind farm to stabilize.

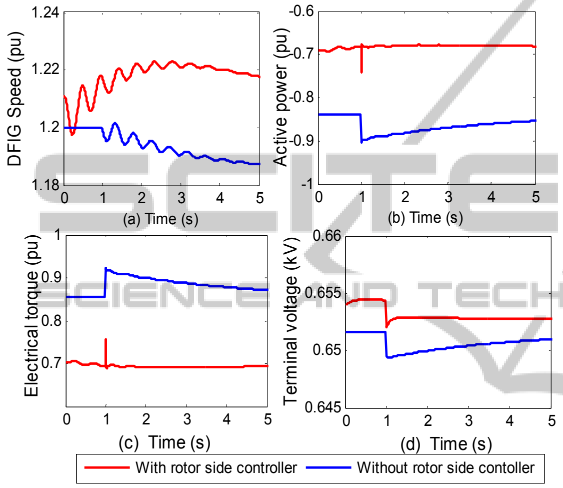


Figure 9: The response of (a) DFIG speed (b) Active power, (c) Electrical torque (d) Terminal voltage to 20% step change in local load at 1s.

The response of the wind farm to different fault type of duration 200ms was investigated. The fault considered are three phase fault, two phase to ground fault, phase to phase fault and single phase to ground fault. The fault was created at 1s at the middle of 100km, 400kV line. The results are presented in figure 9. The severity of the impact of these faults is in the order listed in the legend. This is evident in the speed, the active power, the electrical torque and the rotor current in figure 10. The speed of the generator is limited by the pitch angle. The first swing of the rotor current reached a value of 2pu from the prefault value of 0.8pu for a three phase fault, 1.5pu for two phases to ground fault, 1.3pu for phase to phase fault and 1pu for phase to ground fault.

The response of the wind farm to different fault locations was examined. To get insight into this scenario, a three phase fault of 200ms duration was created at different location on the 50km, 20kV line. The result is shown in figure 11. From the result, the impact of fault at different location has almost the same impact on the response of the wind farm. However, the impact is visibly different at the PCC. The closer the fault location to the PCC, the more the dip in voltage and the more the deviation from the nominal grid frequency.

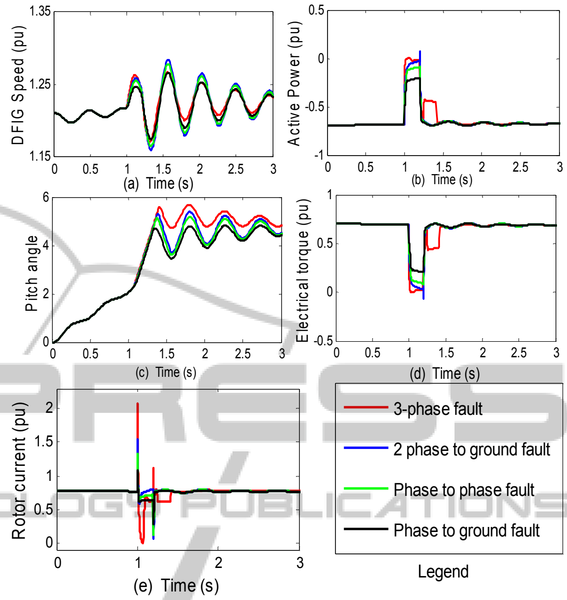


Figure 10: Response of the wind farm (a) speed (b) Active power (c) pitch controller (d) Turbine power (e) rotor current to different types of fault.

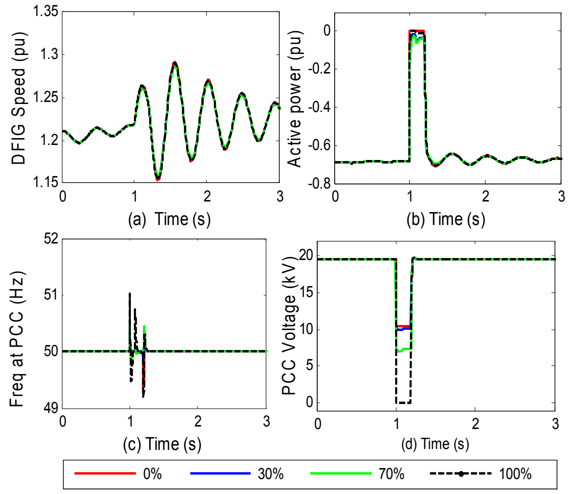


Figure 11: Response of (a) DFIG speed (b) DFIG active power (c) PCC frequency and (d) PCC voltage to 3 phase fault (200ms duration) at different location on the 20kV line.

Figure 12 shows the response of the wind generator with different rotor inertia to a three phase fault created at the middle of 400kV line. The effect of inertia can be noticed in the speed of the generator. The generators with larger inertia are more stable in case of fault compared to the generator with smaller inertia. The first swing in rotor speed for $50kgm^2$ is 1.28pu, 1.26pu for $100kgm^2$, 1.24pu for $150kgm^2$ and 1.22pu for $200kgm^2$ No distict difference in the response of the active power, electrical torque and the terminal voltage are seen.

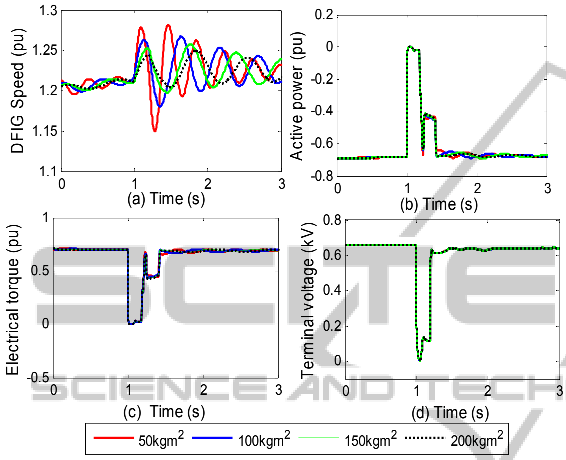


Figure 12: Wind farm with DFIG of different inertia.

The effect of a loss of transmission line (TL) and generation was studied. For the TL, the circuit breaker at both ends of the lines were opened at 1s for the 400kV, 100km line and then for 20kV, 50km line. The circuit breaker at bus 4 connecting the synchronous generator (SG) to the bus was opened at 1s to disconnect the SG from the power system. The results are shown in figure 13. A loss of line causes a surge in the system frequency at the PCC, this caused a reduction of active power to the network by the WF to restore the frequency to the prefault value. The 20kV, 50km line has a severe impact compared to the 400kV, 100km line due to close proximity to the WF. At the instant the SG (generation) was lost; a sudden dip in the system frequency was experienced, this in turn resulted into an instant injection of active power from the WF to the grid to restore the system frequency. The terminal voltage reduces from the prefault value of 0.655kV to a new value of 0.638kV, 0.641kV and 0.650kV for the loss of 50km line, 100km line and SG respectively as a result of change in the system configuration.

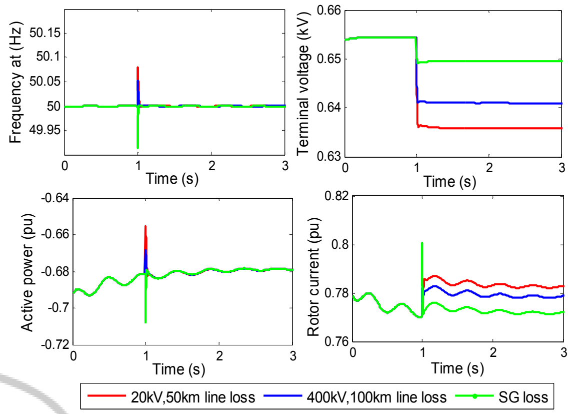


Figure 13: Response to loss of transmission line.

## 5 CONCLUSIONS

The behaviour of wind farm consisting of DFIG in response to different disturbance emanating from the power system has been studied. From the study, the effect of the rotor controller on the stability of a wind farm has been shown to be significant to the stability of the wind farm following a disturbance. Without controller, prefault condition was achieved after about 3s. With controller, the prefault condition was achieved almost immediately.

The type of fault on the power system has different significant impact on the behaviour of the wind farm with three phase fault being the most severe fault. The location of the fault occurence is seen to have little effect on the wind farm. However the location of fault occurence has significant effect on the frequency and the voltage at the PCC.

The inertia of wind generators has influence on the response of the WF to a disturbance. The larger the inertia the lesser the magnitude of oscillation of the generator speed. A larger inertia enhances good stability. The WF responds to the sudden loss of transmission line and generation in such a way as to restore the system frequency. The rotor current and the terminal voltage assume a new value due to the change in the network configuration.

This paper is useful to the ultility operators in understanding the probable response of a wind farm during disturbance in the power system.However, a qualitative study mainly is carried out on a small test system. Further investigation is necessary for a large power system.

## REFERENCES


Arifujjaman, M. D., M. T. Iqbal, et al. (2009). Vector Control of a DFIG Based Wind Turbine, "*Journal Of Electrical & Electronics Engineering.*" 9(2):1057-1066.

Conroy, J. and R. Watson (2009). "Aggregate Modelling of Wind Farms Containing Full-Converter Wind Turbine Generators with Permanent Magnet Synchronous Machines: Transient Stability Studies." *IET Renewable Power Generation* 3(1): 39-52.

El-Sattar, A. A., N. H. Saad, et al. (2008). "Dynamic Response of Doubly Fed Induction Generator Variable Speed Wind Turbine Under Fault." *Electric Power Systems Research* 78: 1240-1246.

El-Sayed, M. A. (2010). Integrating Wind Energy into Weak Power Grid Using Fuzzy Controlled TSC Compensator. *International Conference on Renewable Energies and Power Quality* (ICREPQ,'2010), Granada, Spain.

El-Sayed, M. A. and M. S. Adel (2010). Wind Energy-Grid Stabilization using a Dynamic Filter Compensator. *International Conference on Renewable and Power Quality* (ICRPQ 2010), Spain.

Eping, C., J. Stenzel, et al. (2005). Impact of Large Scale Wind Power on Power System Stability. *5th International Workshop on Large-Scale Integration of Wind Power and Transmission Networks for Offshore Wind Farms*, Glasgow, Scoland.

Folly, K. A. and S. Sheetekela (2009). Impact of fixed and variable speed wind generators on the transient stability of a power system network. *Power Systems Conference and Exposition*, 2009. PSCE '09. IEEE/PES.

Krause, P. C., O.Wasynczuk, et al., Eds. (2002). *Analysis of Electric Machinery and Drive Systems Second Edition*, A John Wiley and Sons,Inc.Publication.

Lipo, T. A. (2000). *Electric Machine Analysis and Simulation. Research Report.* W. E. M. a. P. E. Consortium. Madison, Wisconsin Power Electronic Research Center, University of Wisconsin-Madison.

Naimi, D. and T. Bouktir (2008). "Impact of Wind Power on the Angular Stability of a Power System." *Leonardo Electronic Journal of Practices and Technologies* 12: 83-94.

Poller, M. A. (2009). *Doubly_FEd Induction Machine Models for Stability Assessment of Wind Farms,* http://www.digsilent.de/consulting/publication/DFIG modelling date accesed, 28th Sept.

Slootweg, J. G., S. W. H. de Haan, et al. (2001). Modeling wind turbines in power system dynamics simulations. *Power Engineering Society Summer Meeting,* 2001. IEEE.

Soares, O. M., H. N. Gocalves, et al. (2009). Analysis and NN-Based Control of Doubly Fed Induction Generator in *Wind Power Generation. International Conference on Renewable Energies and Power Quality* (ICREPQ'2009), Valencia(Spain).

Veganzones, C., S. Martinez, et al. (2005). Large Scale Integration of Wind Energy into Power Systems. *Electrical Power Quality and Utilisation, Magazine.* Spain. 1: 15-22.

Xing, Z., Q. Zheng, et al. (2005). "Integration of Large Double-Fed Wind Power Generator System into Grid." *8th international Conference on Electrical Machines and System.*: 1000-1004.


## APPENDIX

TABLE: DFIG Parameters.

| Description | Values |
|---|---|
| Active power ,P | 2MW |
| Rated voltage | 0.69kV |
| Stator resistance Rs | 0.01pu |
| Stator reactance, Xs | 0.1pu |
| Rotor resiatance, Rr | 0.01pu |
| Rotor reactance, Xr | 0.1pu |
| Magnetizing reactance,Xm | 3.5pu |
| Inertia | 75Kgm$^2$ |